PHILOSOPHICAL TRANSACTIONS OF THE ROYAL SOCIETY A MATHEMATICAL, PHYSICAL & ENGINEERING SCIENCES

The infrared predissociation spectrum of H_3^+

Faye Kemp, C. Euan Kirk and Iain R. McNab

Phil. Trans. R. Soc. Lond. A 2000 **358**, 2403-2418
doi: 10.1098/rsta.2000.0656

10.1098/rsta.2000.0656

The infrared predissociation spectrum of H_3^+

By Faye Kemp, C. Euan Kirk and Iain R. McNab

Department of Physics, University of Newcastle upon Tyne, Newcastle upon Tyne NE1 7RU, UK

Experimental measurements of the infrared predissociation spectrum of the H_3^+ ion are briefly reviewed. The spectrum involves states between $-1100\ cm^{-1}$ and above $+2000\ cm^{-1}$ of the dissociation limit into $H^+ + H_2$. Over 26 000 lines were seen in the wavenumber range 872–1094 cm^{-1}.

Keywords: clumps; dissociation; H_3^+; infrared; ion beam; isotopomer

1. Introduction

In this paper we review the experimentally determined properties of the H_3^+ infrared predissociation spectrum, and other experimental measurements relevant to this spectrum. A brief review of theory relevant to the infrared predissociation spectrum of H_3^+ up to 1993 can be found in Carrington *et al*. (1993), and the current state of such theory is discussed by Tennyson (this issue). A comprehensive review of the spectroscopy of H_3^+ up to 1995 was given by McNab (1995), and a review of the spectroscopy of ion beams was given by Cox *et al*. (1999).

The predissociation spectrum of H_3^+ near its dissociation limit was measured by Carrington and his co-workers and reported in three papers (Carrington *et al*. 1982, 1993; Carrington & Kennedy 1984), and we now review the experimental findings; for reasons of space these papers will not be referenced again. The spectrum was observed in the infrared between 872 and 1094 cm^{-1} and arose from the process

$$H_3^+ + h\nu\ (\text{infrared}) \rightarrow (H_3^+)^* \rightarrow H^+ + H_2,$$

where $h\nu$ represents a photon.

The spectrum of an ion beam of H_3^+ was detected by monitoring the production of H^+ fragment ions as a function of frequency. The photon energy was a small fraction of the dissociation energy of ground state H_3^+ ($D_0 = 49\,590\ cm^{-1}$), and therefore probed highly excited states of H_3^+ in the ion beam. In order to orient the reader, figure 1 shows the significant energies of H_3^+ and indicates the range believed to be involved in the predissociation spectrum. The predissociation spectrum contained nearly 27 000 transitions in the 222 cm^{-1} interval. The most intense lines in the spectrum were found to appear in four clumps with an average separation of 52.6 cm^{-1}. Less-detailed studies of similar spectra of the isotopomers D_3^+, H_2D^+ and D_2H^+ have also been made. The D_3^+ spectrum was essentially similar to the H_3^+ spectrum, with a higher density of lines as expected. The mixed-isotope species displayed similar highly congested spectra with the additional complication that spectra obtained by monitoring fragment H^+ and fragment D^+ ions were different.

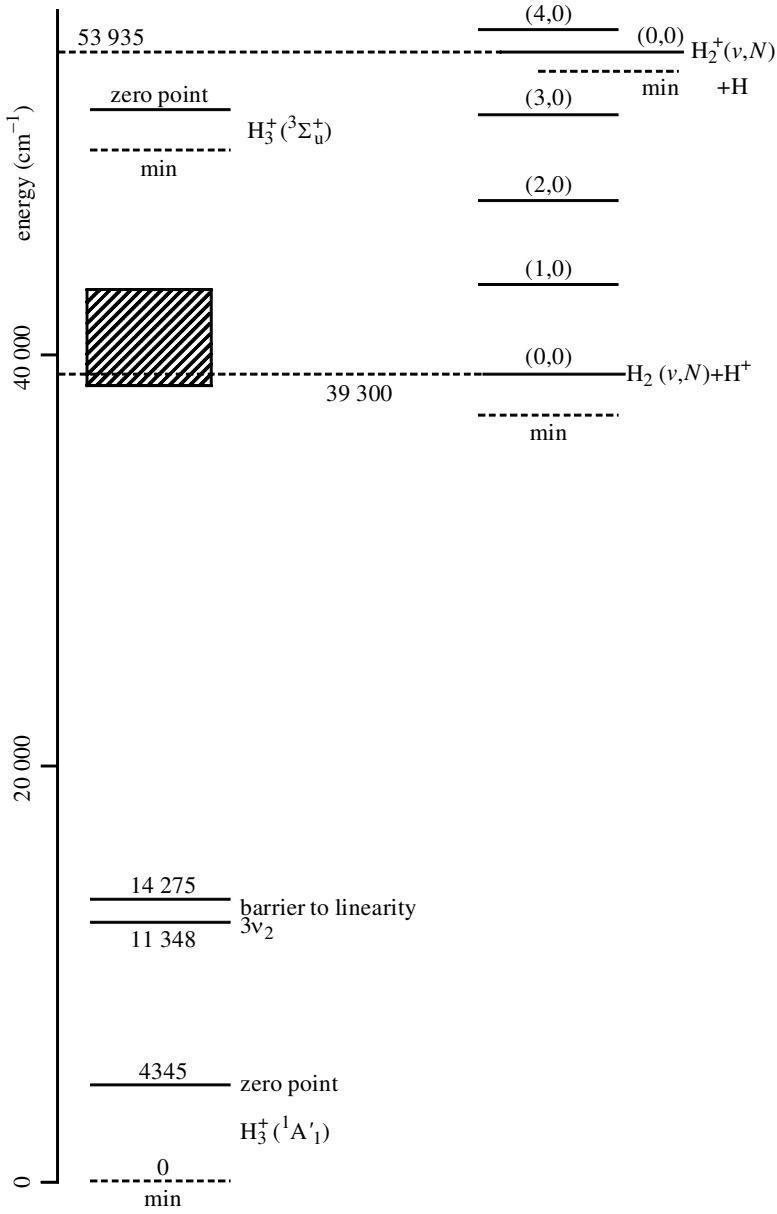

Figure 1. An energy diagram showing significant energies of H_3^+. The hatched range of energies is that believed to contribute to the predissociation spectrum.

2. Experiment

Most measurements of the H_3^+ predissociation spectrum were accomplished with a single fast-ion-beam/laser-beam spectrometer. As the geometry of the instrument imposed crucial limitations on the data, it is now described in some detail.

The ion-beam machine used was a modified Vacuum Generators ZAB-1F reverse-geometry tandem mass spectrometer (hereafter referred to as the ZAB), the main

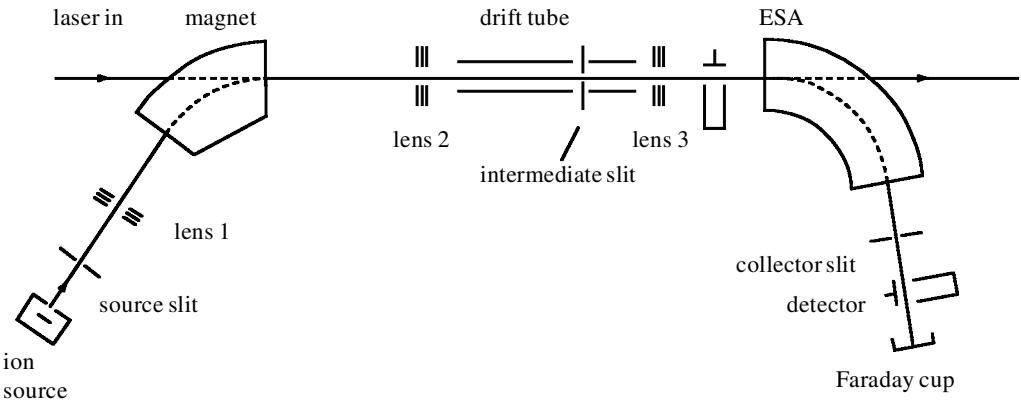

Figure 2. A schematic of the apparatus: gas was admitted into the ion source, ionized, and the magnetic sector used to select H_3^+ by its m/q value. The drift-tube area was irradiated with a carbon dioxide laser and the resultant H^+ fragments selected by the ESA. Spectra were obtained by scanning the source potential (and magnet), while monitoring the number of H^+ fragments.

features of which are illustrated in figure 2. The parent ions, generated in an electron-impact ion source, were accelerated by a positive potential and mass selected. Transmitted ions were brought to a focus at an intermediate slit situated within a Faraday cage (hereafter called the drift tube). An infrared laser beam was coaxial with the ion beam and induced fragmentation of H_3^+. The fragments formed in the drift tube were selected according to their kinetic energy by an electrostatic analyser (ESA) and detected by an electron multiplier. Spectra were recorded by measuring changes in the number of ions formed in the drift tube with changing effective laser frequency (changing ion-beam potentials).

The production of H_3^+ (or D_3^+, D_2H^+, H_2D^+) was by the introduction of molecular hydrogen (or deuterium, or a mixture of both) into an electron-impact ion source. The pressure outside the source was *ca.* 10^{-4} Torr, and the internal pressure was estimated to be 10^{-3} Torr.

Two ion sources were used in the work; both were manufactured by Vacuum Generators Analytical. The first was a standard electron-impact/chemical-ionization source that employed a geometry in which the ions were extracted in a direction perpendicular to the electron beam used to cause ionization. The second was an 'in-line' electron-impact ion source, in which the ionizing beam of electrons was collinear with the extracted ion beam. The in-line ion source gave a beam current about three times greater than the standard source. It was possible to vary the source potential from 0 to +10 kV and the ions were accelerated from the source by collecting and collimating slits at earth potential. Typically, beam currents of H_3^+ of greater than 10^{-7} A were employed.

After extraction of all ions from the ion source, a parent ion beam was selected by its mass-to-charge ratio using a magnetic analyser, which was set to transmit the parent ion of interest (and all other ions with the same mass-to-charge ratio).

The parent ion beam then passed through the drift tube, within which it interacted with a laser beam; both beams were brought to a focus at an intermediate slit. Spectroscopic transitions in H_3^+ were driven by a line-tunable infrared continuous-wave carbon dioxide laser (an Edinburgh Instruments PL3 or PL4). The laser beam was

admitted into the apparatus by means of zinc selenide windows and aligned coaxially with the ion beam. The laser beam was aligned either co-propagating (parallel) or counter-propagating (antiparallel) to the ion beam. The laser beam was focused with a zinc selenide lens.

The infrared laser frequency experienced by the H_3^+ ions was scanned by altering the beam potential (accelerating potential). This was equivalent to a frequency scan, as a change in beam potential produced an alteration in velocity, and via the Doppler effect this became a frequency change. Thus, the velocity of the resonant ion was translated into a resonant frequency by the equation:

$$f_{\mathrm{res}} = f_{\mathrm{laser}} \left(\frac{1 \mp v/c}{1 \pm v/c} \right)^{1/2},$$

where v is the speed of the ion, the upper signs refer to co-propagating ('parallel') beams, and the lower signs refer to counter-propagating ('anti-parallel') beams.

The spectroscopic transitions in H_3^+ were detected by observing the increase in H^+ fragments when the effective laser frequency was resonant with a transition. A cylindrical-plate ESA was used to separate off the H^+ fragments from the drift tube. By applying a DC bias electric potential of up to ± 500 V to the drift tube, fragment H^+ ions could be 'labelled' by a kinetic energy different to those formed in a region of earth potential. The kinetic energy resolution of the ESA was sufficient that it could be set to transmit only the H^+ fragments produced within the drift tube. Therefore, only the transitions that occurred in the drift tube were monitored, and this enabled transitions to be recorded without also recording the non-resonant photofragment background. The H^+ current was monitored with an off-axis electron multiplier situated after the ESA.

The H^+ current from the off-axis electron multiplier was converted to a voltage and processed by a lock-in amplifier. Two modulation schemes were used in this work.

(1) Frequency modulation (FM) was achieved by applying a square-wave voltage of 0–10 V at a frequency of 0–10 kHz to the drift tube, which (via the Doppler effect) was equivalent to frequency modulation; the demodulated signal therefore produced first-derivative line shapes. The frequency-modulation scheme discriminates against broad lines and, therefore, against any non-resonant photofragment background. FM was used for most work due to its higher sensitivity despite the significant undermodulation of broad lines that may have been caused.

(2) Amplitude modulation (AM) was achieved by laser chopping and resulted in demodulated signals with a normal absorption line shape. Amplitude modulation does not discriminate against broad lines, but modulates any non-resonant photofragment background, and is therefore less sensitive than frequency modulation.

3. Experimental results

The infrared predissociation spectrum of H_3^+ was recorded from 872.120 cm^{-1} to 1094.006 cm^{-1} and over 26 500 lines were measured in this range. Small gaps in the range were incurred because of the lack of suitable laser lines. A typical spectrum obtained by laser chopping is shown in figure 3.

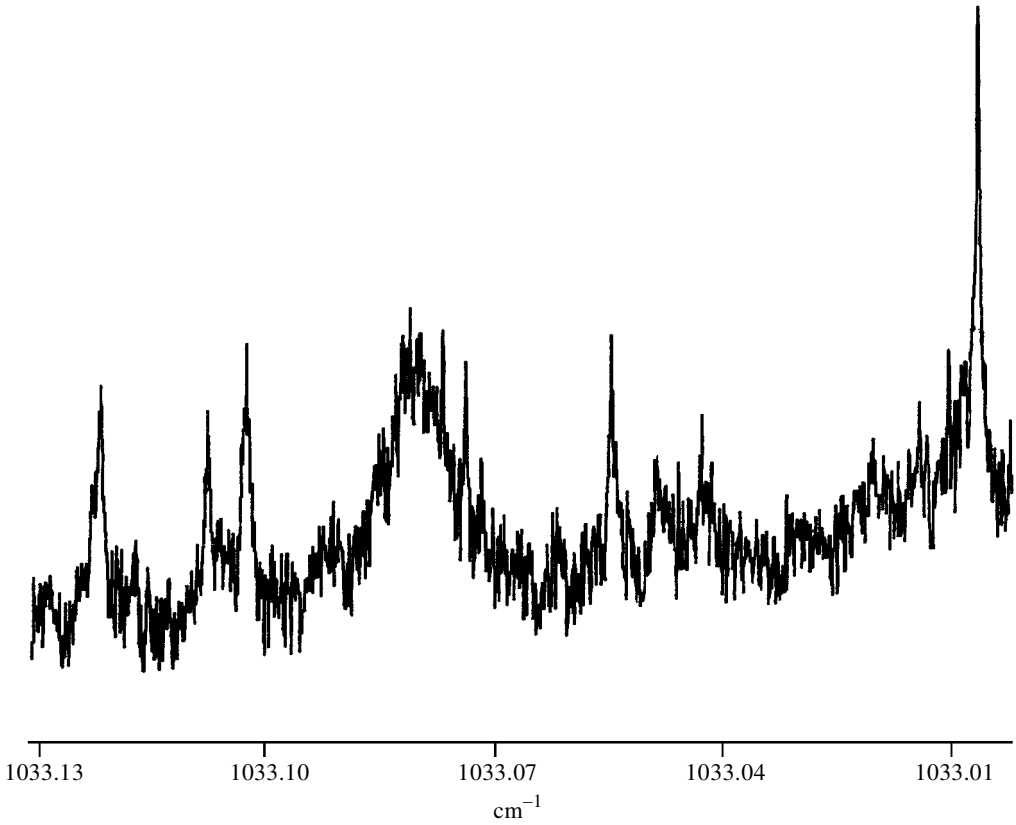

Figure 3. A typical H_3^+ spectrum obtained by laser chopping. The widely varying linewidths are a good indication that the spectrum involves predissociating states.

(*a*) *Reproducibility of the spectrum*

The reproducibility of the spectrum was demonstrated by the use of different laser lines under different orientations and different drift-tube potentials. Typically, scans taken under different conditions gave line positions that were reproducible to within 0.001 cm^{-1}. To demonstrate that the spectrum was not machine dependent, a test with a second ion-beam machine (described in detail by Carrington *et al.* (1989)) was carried out. This instrument was used with an in-line ion source, but has a much shorter total ion path and uses two magnetic sectors, in contrast to the ZAB, which uses one magnetic sector and then an electric sector for kinetic energy analysis. Doppler tuning was achieved by applying a scanning potential to the drift tube. A number of regions of the H_3^+ spectrum were examined with both instruments and the spectral lines were found to be convincingly reproducible in both frequency and relative intensity.

(*b*) *Limitations of the experiment*

The experiment had two major limitations.

(1) The first limitation was that, despite the expected long-term benefits of the very-high-resolution data obtained, it was not possible to produce a low-res-

olution form of the entire spectrum. Computer convolution techniques were employed to produce a pseudo-low-resolution spectrum.

(2) The second limitation was that it was not possible to have a truly standard set of conditions for recording the spectrum. The ion-beam intensity was dependent upon the beam potential; the collection efficiency of the ESA was dependent upon the centre of mass kinetic energy of the H^+ ions; and the modulation amplitude should strictly have been maximized for each line according to its natural width.

To overcome limitation (1), computer convolution techniques were employed to produce a pseudo-low-resolution spectrum. To overcome limitation (2), a compromise set of conditions was used in the initial work as follows: laser powers of 7 ± 3 W, scan rate of $1\ \mathrm{V\ s^{-1}}$ (*ca.* $0.45\ \mathrm{cm^{-1}\ h^{-1}}$), frequency modulation at a modulation amplitude of 7 V. The ratio of ESA potential to source potential was set to maximize the collection efficiency for protons with zero kinetic energy release. Even with these limitations on the variables, the entire H_3^+ spectrum took 2500 h to record, and, hence, attention was initially focused upon the stronger lines only. Unfortunately, at 7 W many lines in the spectrum were saturated and relative intensities in the initial measurements may not have been representative of absolute transition strengths.

(*c*) *Nature of the spectrum*

The resonance lines within the spectrum were detected by an increase in the number of H^+ fragment ions at the electron multiplier, which arose from predissociation of H_3^+. Three mechanisms to explain the creation of these fragments from the parent H_3^+ ion beam were initially considered. These were (a) collision-induced dissociation by the background gas within the drift tube (mostly hydrogen from the source); (b) direct photodissociation; and (c) predissociation. Further observations ruled out suggestions (a) and (b). The spectrum arises from the resonant predissociation

$$H_3^+ + h\nu \rightarrow (H_3^+)^* \rightarrow H^+ + H_2(v, N).$$

Consequently, the spectrum contains lines with many different widths corresponding to the natural lifetimes of the predissociating states. There was no means of determining the vibration (v) or rotation (N) quantum states of the H_2 fragments produced.

The possibility that the spectrum arose through two-photon photodissociation processes was also investigated. It was found that integrated signal strengths were linearly dependent upon laser power, as expected for a single-photon process. It was also found that the strongest lines in the spectrum were saturated at laser powers of more than 2 W.

(*d*) *Lifetimes of the resonant levels*

The geometry of the experiment placed natural constraints on the lifetimes of the initial and final states that could be observed. In order for an initial state to be involved in a transition, its lifetime had to be sufficiently great that it survived extraction from the ion source and transport to the drift tube ($\tau_{\mathrm{init}} > 3\ \mu\mathrm{s}$). Conversely, a final-state lifetime had to be sufficiently short that predissociation could

occur within the time of flight through the drift tube ($\tau_{\text{final}} < 0.7\ \mu\text{s}$). Very short final-state lifetimes led to broad lines, which were unlikely to be observed and placed a limit of $\tau_{\text{final}} > 7$ ns.

The window on the lifetimes of the initial and final states is an important constraint for all theories of predissociation. The lifetime of the final state of a transition is directly measured from the observed linewidth; systematic measurements of linewidths are discussed below.

The measurement of initial-state lifetimes was not possible, in general, but could be measured directly for some transitions. In altering the time of flight of an initial state from the ion source to the drift tube, three possible outcomes were expected:

(i) no change in line intensities would result due to the marginal time delay caused;

(ii) that the initial state would have decayed more before the ions reached the drift tube, yielding a weaker line intensity;

(iii) that the time spent inside the drift tube increased, and, hence, final-state fragmentation increased, yielding a stronger line intensity.

A small search of the available wavenumber range showed that most lines obeyed hypothesis (i), since the changes in time that were produced were small. However, eight examples of type (ii) behaviour were observed; no lines showed type (iii) behaviour. For the eight examples of type (ii) behaviour, first-order kinetics was used to obtain lifetimes from two measurements of the line intensity at high and low source potentials (where the spectra were obtained with different laser lines and/or orientations). All initial-state lifetimes that were measured in this manner were in the range 1.1–2.3 μs.

(*e*) *Photofragment proton kinetic energies*

Photofragment H^+ ions were found with kinetic energy releases of up to 3000 cm^{-1} (three times the photon energy). The ESA was used to select the H^+ fragments by their kinetic-energy-to-charge ratio. The resolution of the instrument was sufficient to measure the centre-of-mass kinetic energy of the fragment protons for each resonant predissociating transition; many lines had kinetic energy releases of up to 3000 cm^{-1}. Power studies showed that no multi-photon processes occurred, and as the photon energy was between 870 and 1090 cm^{-1}, it was proved that many lines in the predissociation spectrum arose from transitions in which both the upper and lower energy levels lay at least 2000 cm^{-1} above the lowest dissociation limit to $H_2(v, N) + H^+$.

(*f*) *Clumping of intense transitions*

The most intense lines in the spectrum fall in four distinct equally spaced clumps. A full recording of the H_3^+ spectrum was made by collecting H^+ fragments with the ESA set at zero kinetic energy release, using the standard conditions listed above, and almost 27 000 lines were located. No traditional spectroscopic analysis was possible of the full dataset. In order to begin a spectroscopic analysis, it is usual to take a low-resolution spectrum as a starting point, but this was not possible with the apparatus available. To try and aid understanding, pseudo-low-resolution spectra were generated from the high-resolution data using computer convolution with a Gaussian

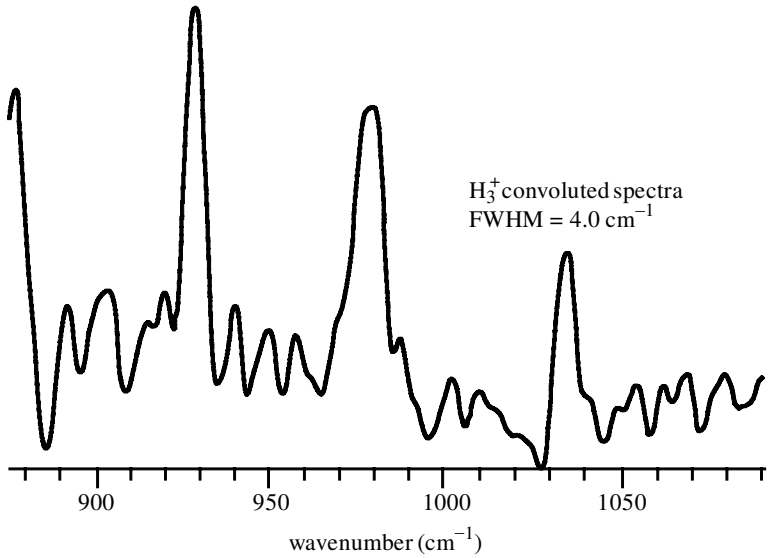

Figure 4. A pseudo-low-resolution spectrum produced by a computer convolution of the 1934 strongest lines in the spectrum with a Gaussian function with a full-width half-maximum of 4 cm^{-1}.

function with a full-width half-maximum of 4 cm^{-1}. This method lost the contribution that would have been made to a low-resolution spectrum by broader lines, as these were undermodulated, as previously described. As a simplification, a further convolution was calculated from the 1934 lines with a signal-to-noise ratio greater than 14:1, and this convolution is shown in figure 4. The pseudo-low-resolution spectrum showed four clear peaks due to clumps of high-intensity lines. The average separation of the peaks was 52.6 cm^{-1}. The average separation between the peaks showed good correlation with $\Delta N = 2$ transitions in the first four vibrational levels ($v = 0, 1, 2, 3$) of H_2 (Wolniewicz 1983), and it was suggested that H_3^+ near predissociation might be considered as an $H_2 \cdots H^+$ complex in which the vibrational (v) and rotational (N) quantum numbers of the H_2 were largely conserved.

(*g*) *Detailed measurements of the clump at* 1033.62 cm^{-1} (1025–1045 cm^{-1})

The $H_2 \cdots H^+$ model was disproved by remeasuring the 1033.62 cm^{-1} clump using laser powers at which transitions were not saturated. Pfeiffer & Child (1987) calculated the H_3^+ spectrum assuming the $H_2 \cdots H^+$ model and were unable to account for intensity above 1025 cm^{-1} unless the spectrum was saturated. The spectral region 1025–1045 cm^{-1} was therefore remeasured with a laser power of 2 W, which was known not to cause saturation. It was found that the intense lines in this region could still be detected at these low powers, thus disproving the $H_2 \cdots H^+$ model for H_3^+ at dissociation.

The spectra were recorded using amplitude modulation in order to simultaneously study the unbroadened linewidths and, hence, the lifetimes of the final states in the transitions. The linewidths of the transitions (and, hence, the final-state lifetimes) were studied as a function of frequency (see figure 5). As expected, the final-state

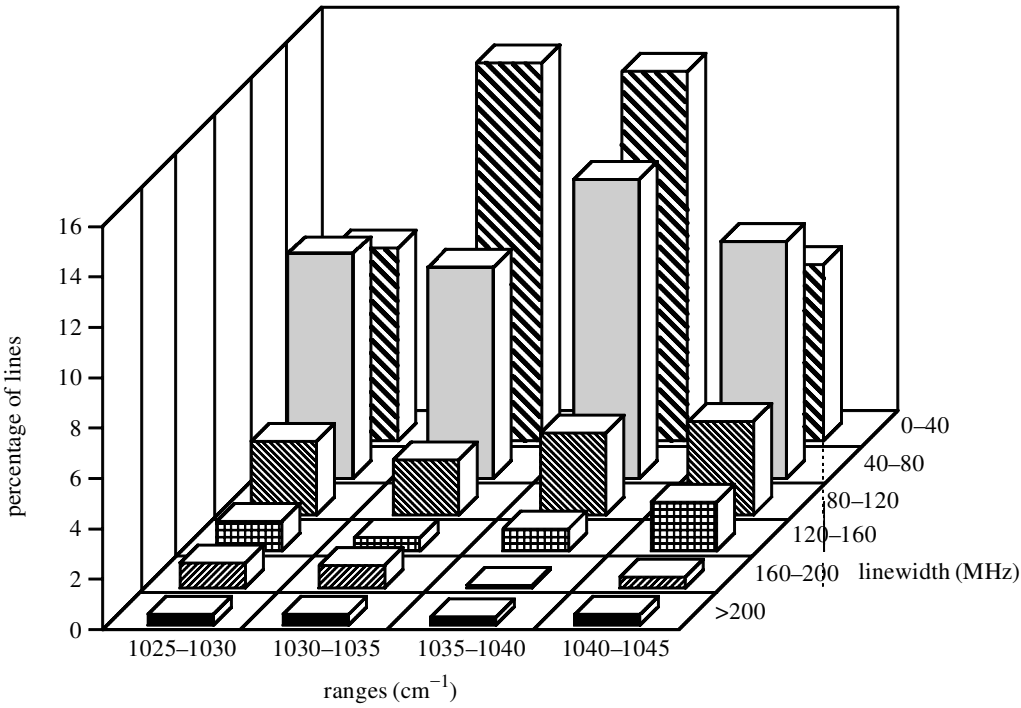

Figure 5. A bar chart illustrating the distribution of linewidth (MHz) for the 265 lines in the 1025–1045 cm^{-1} range.

lifetimes were in the range 5×10^{-10} to 2×10^{-8} s. It was found that the highest intensity lines at the centre of the clump had the smallest linewidths (greatest lifetimes). The outer regions of the clump had a higher proportion of broad lines.

(*h*) *Detailed measurements of the clump at* 978.45 cm^{-1} (964.0–991.6 cm^{-1})

An important conclusion to be drawn from theory (Miller *et al*. 1989), which was largely verified, was that the intense lines in the clumps arose from transitions with small kinetic energy releases, and that small kinetic energy releases were directly correlated with H_3^+ states of low angular momentum. Spectra were re-examined to determine if the most intense lines in the clump had low kinetic energy release. The clump at 978.45 cm^{-1} was re-examined by recording spectra over the range 964.0–991.6 cm^{-1}, the ESA was used as a kinetic energy window that could be set to transmit protons with (average) centre-of-mass kinetic energies within a selected range. Some of the stronger, low kinetic energy release lines were also examined by scanning the ESA while a constant beam potential was used to drive the transition; an example of such a scan is shown in figure 6.

Figure 7 shows examples of typical spectra obtained in different kinetic energy windows. For a kinetic energy window centred at 0 cm^{-1} (figure 7*a*), lines with a range of widths and intensities were observed with no identifiable pattern (*ca.* 17 per cm^{-1} with signal-to-noise ratios of at least 10). A kinetic energy window centred at 500 cm^{-1} (figure 7*b*) gave a large number of weak lines (*ca.* 60 per cm^{-1}) of varying widths and intensities. Using a kinetic energy window centred at 3000 cm^{-1} (fig-

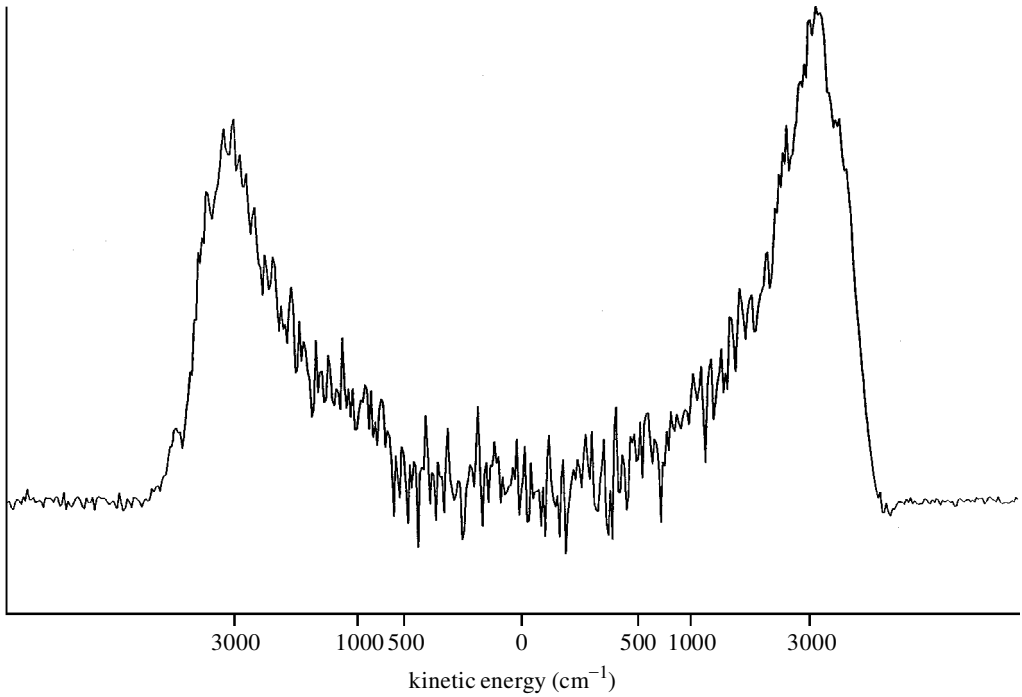

Figure 6. A kinetic energy scan using the ESA, at a fixed beam potential of 5088 V. Transition is that at wavenumber 983.6166 cm^{-1} within the 978.45 cm^{-1} clump.

ure 7*c*), spectra with low-intensity background but with a number of strong lines (or clusters of lines) well separated from each other were obtained. Again, no discernible pattern was evident.

Detailed measurements were made of spectra using kinetic energy release windows centred at 0, 50, 100, 500 and 3000 cm^{-1}. It was found that the majority of the strongest lines were formed at very low kinetic energy, confirming the theory. Detailed comparison of a number of scans performed using both methods confirmed the consistency of the measurements.

(*i*) *Investigations of* D_3^+, HD_2^+, H_2D^+

There was no difficulty in forming parent beams of the deuterium isotopomers, and the predissociation spectrum could be measured in an analogous manner to the H_3^+ spectrum:

$$\begin{aligned} D_3^+ + h\nu &\rightarrow (D_3^+)^* \quad \rightarrow D^+ + D_2, \\ H_2D^+ + h\nu &\rightarrow (H_2D^+)^* \quad \rightarrow H^+ + HD \text{ or } D^+ + H_2, \\ HD_2^+ + h\nu &\rightarrow (HD_2^+)^* \quad \rightarrow H^+ + D_2 \text{ or } D^+ + HD. \end{aligned}$$

Spectra of D_3^+ were more dense than the H_3^+ spectra and about five times weaker, presumably because the same population was distributed over more levels. For the mixed-isotope species, the spectra could be monitored by either the H^+ or D^+ fragmentation channel. Spectra of HD_2^+ obtained at zero kinetic energy release through

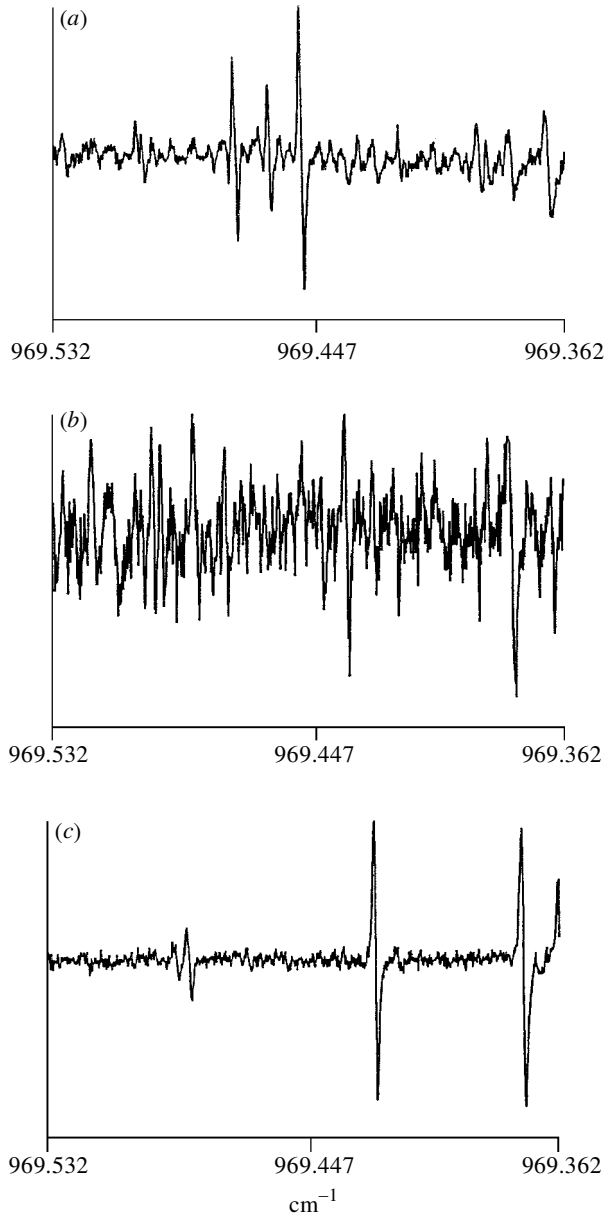

Figure 7. A section of the 978.45 cm^{-1} clump recorded using three different kinetic energy windows centred at (*a*) 0 cm^{-1}, (*b*) 500 cm^{-1}, and (*c*) 3000 cm^{-1}.

the two different channels over the same frequency range appear completely different and, therefore, represent different sets of transitions. Similar measurements of the spectrum of H_2D^+ were more difficult because it was not possible to distinguish between H_2D^+ and D_2^+ with the magnetic analyser. Since D_2^+ readily undergoes infrared photodissociation (resulting in D^+ fragments with kinetic energies up to that of the photon used (see, for example, Carrington *et al.* 1989)), observations of

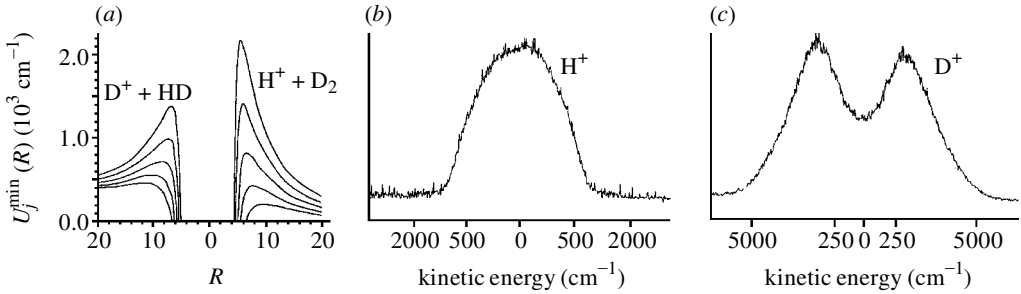

Figure 8. A direct illustration of the different kinetic energy distributions due to predissociation from HD_2^+. The kinetic energy distributions obtained for the two fragmentation channels arise from spontaneous predissociation of the ion beam without laser excitation. The potential barriers for the two limiting dissociation channels are shown in part (*a*) for $L = 20$, 25, 30, 35 and 40, together with the observed kinetic energy distributions of the two resulting fragments in parts (*b*) and (*c*).

H_2D^+ spectra by the D^+ channel were made against a high non-resonant photofragment background and were, therefore, less sensitive than spectra obtained via the H^+ dissociation channel. To minimize the production of D_2^+ (and, therefore, the non-resonant background), an excess of H_2 was used in the ion source for these measurements.

The dependence of the zero kinetic energy release spectra of the mixed-isotope species upon the fragment used for detection was explained by Berblinger *et al*. (1988, 1989) and was confirmed by Chambers & Child (1988). The difference in the spectra is due to the nature of the angular momentum barriers for the two dissociation channels. Consider HD_2^+; the fragmentation route can be either (1) $D_2 \cdots H^+$ or (2) $HD \cdots D^+$. The total angular momentum barriers can then be approximated by the orbital angular momentum (L) alone, with the appropriate classical potential energy expression $V(R) + L^2/2\mu R^2$, where μ is now the reduced mass appropriate to (1) or (2). The angular momentum barrier in the deuteron channel is always lower than in the proton channel. Quantum mechanically, we must also consider the difference in zero-point energies between D_2 and HD, and the difference in ionization potential between H and D. Allowing for these differences shifts the barriers to the positions shown in figure 8*a*. The specific conclusions for HD_2^+ and H_2D^+ were as follows: for H_2D^+, protons should have kinetic energy less than 1190 cm^{-1} and deuterons should have kinetic energy greater than 540 cm^{-1}; for HD_2^+, protons should have kinetic energy less than 680 cm^{-1} and deuterons should have kinetic energy greater than 286 cm^{-1}.

To verify this argument, spectra of the mixed isotopomers detected using both H^+ and D^+ fragments were recorded using a range of kinetic energy windows. For H_2D^+ it was found that kinetic energy releases of H^+ fragments were predominantly less than 1200 cm^{-1}, while energy releases of D^+ fragments were predominantly located in windows centred at 500 and 1200 cm^{-1}. For HD_2^+, most D^+ fragments appeared in the 300–750 cm^{-1} kinetic energy release range, although transitions were still abundant in the 1500 and 3000 cm^{-1} windows. Most of the lines observed monitoring H^+ fragments were concentrated in the 0 and 300 cm^{-1} windows. Due to the high density of weak lines observed in the intermediate kinetic energy ranges for both of the mixed-isotope species, it was impossible to identify single transitions

PHILOSOPHICAL TRANSACTIONS OF THE ROYAL SOCIETY A MATHEMATICAL, PHYSICAL & ENGINEERING SCIENCES

that could be detected by monitoring both H^+ and D^+ fragments. The observations agree well with the theoretical predictions. It was also found that fragments arising from spontaneous predissociation of the parent ion beams yielded fragments with the expected kinetic energy releases, and this is illustrated in figure 8 (parts (*b*) and (*c*)).

(*j*) *Multiple dissociation channels*

Studies of kinetic energy scans recorded while driving a transition at a fixed ion-beam potential showed that more than one scattering pattern can be observed, with different kinetic energy releases. This showed that the fragmentation of H_3^+ took place via different channels connected with the vibration–rotation energies of the fragment H_2 molecule. The constancy of the relative intensities of such peaks when the scan was reproduced at different source pressures (which might be expected to result in different relative populations of levels) or slightly different ion-beam potentials (which checked that the two transitions occurred at exactly the same transition frequency) confirmed that genuine examples of competitive predissociation through two different channels had been found.

(*k*) *Spectra at dissociation obtained at higher excitation frequencies*

A few weak lines of the H_3^+ predissociation spectrum were obtained using a CO laser at a frequency of 1860 cm^{-1}. Preliminary searches for predissociation spectra of H_3^+ in the visible were unfruitful (P. J. Sarre, personal communication).

(*l*) *Excitation mechanisms of the* H_3^+ *beam*

The reaction leading to the production of H_3^+ in the ion source (see, for example, Badenhoop *et al.* (1987), and references therein) is thought to be

$$H_2 + e^- \rightarrow H_2^+ \ (v = 0\text{–}19) + 2e^-,$$
$$H_2 + H_2^+ \ (v = 0\text{–}19) \rightarrow H_3^+ + H.$$

This fundamental reaction is still of great interest and relative cross-sections have been reported for reactions involving state-selected H_2^+ (Softley *et al.* 1997). Crossed molecular beam studies (Gentry *et al.* 1975; Anderson *et al.* 1981) strongly suggest that the product H_3^+ ions possess high internal energies. Potential gradients within an ion source may accelerate H_2^+ ions to energies of several eV before reactive collision with H_2 occurs, and Gentry *et al.* (1975) showed that translational energy was efficiently converted into internal energy of the H_3^+ product.

In addition to excitation processes that occur directly in the formation of H_3^+, subsequent collisions may be important. Cross-section measurements (Peko & Champion 1997) show that at low energies (less than 5 eV) collisions between H_3^+ and H_2 result predominantly in proton-transfer reactions and lead to a highly excited H_3^+ product that often autodissociates. As H_3^+ ions were extracted from the ion source they were rapidly accelerated to 1–10 keV and could collide with H_2 effusing from the ion source.

To maximize production of H_3^+, ion sources are normally used at fairly high pressures. At very high pressures, collisions result in vibrational cooling of H_3^+ (see, for example, Yousif *et al.* 1997). In the production of H_3^+ by a particular ion source (Peko & Champion 1997), there is, therefore, a delicate balance between:

(a) translation of kinetic energy of reactants into internal energy of H_3^+;

(b) de-excitation of H_3^+ in collisions with H_2; and

(c) proton transfer excitation of H_3^+ due to collisions with H_2.

If a different ion source had been used, the predissociation spectrum of H_3^+ might not have been discovered.

4. Future work

Ideally, one would now like to make the following investigations.

(1) A systematic recording of the spectra of all isotopomers of H_3^+ at a variety of kinetic energy releases over the entire accessible wavenumber range.

With the original experiment (which no longer exists), it would have taken hundreds of person-years of effort to generate these data. We are currently designing an experiment that we hope will enable these data to be recorded on a more manageable time-scale.

(2) A search for spectra resulting from transitions between states at dissociation and more regular deeply bound states (i.e. predissociation spectra obtained with higher laser frequencies).

Spectra at CO wavenumbers (1860 cm^{-1}) have been recorded, and might be of further interest. Preliminary searches for predissociation spectra in the visible were unfruitful (P. J. Sarre, personal communication), but further searches will be undertaken.

(3) Systematic measurements of the intensity of H_3^+ spectra using a variety of ion sources, and under a variety of ion-source conditions.

This study will determine whether the predissociation spectrum depends upon (a) the formation of H_3^+; (b) proton extraction reactions of H_3^+ with H_2; or (c) both. We have many ion sources at our disposal, and will undertake more systematic investigations of what ion-source conditions are necessary to produce H_3^+ in highly excited states.

(4) Measurements of relative line intensities in the H_3^+ spectrum when using different mixtures of ortho and para hydrogen in the ion source.

It was suggested by Quack (1977) that para hydrogen will give rise to para-H_3^+; this has been verified for H_3^+ in low energy levels (Uy *et al*. 1997) by measuring the dependence of line intensities on the ratio of para/ortho hydrogen used in a discharge. Similar measurements of line intensities in the predissociation spectrum should give some information about the number of hydrogen-exchange reactions that occur in the ion source, because such reactions destroy para-H_3^+.

5. Conclusion

Experimental measurements of H_3^+ infrared predissociation revealed a dense spectrum that has so far defied traditional spectroscopic assignment, although the quantum mechanics of H_3^+ at dissociation is now well understood (see Tennyson, this issue,

for a summary of theoretical investigations). With modern algorithms and computer power, a full quantum assignment of the spectrum may be possible. The observation of sparse spectra at high fragment kinetic energy releases (corresponding to high angular momentum) may provide a route into a full spectroscopic assignment. When such an assignment is possible, we will know more about the potential energy surface of H_3^+ at dissociation than for any other polyatomic molecule.

References

Anderson, S. L., Houle, F. A., Gerlich, D. & Lee, Y. T. 1981 *J. Chem. Phys.* **75**, 2153–2162.

Badenhoop, J. K., Schatz, G. C. & Eaker, C. W. 1987 *J. Chem. Phys.* **87**, 5317–5324.

Berblinger, M., Gomez Llorente, J. M., Pollak, E. & Schlier, Ch. 1988 *Chem. Phys. Lett.* **146**, 353–357.

Berblinger, M., Schlier, Ch. & Pollak, E. 1989 *J. Phys. Chem.* **93**, 2319–2328.

Carrington, A. & Kennedy, R. A. 1984 *J. Chem. Phys.* **81**, 91–112.

Carrington, A., Buttenshaw, J. & Kennedy, R. A. 1982 *Mol. Phys.* **45**, 753–758.

Carrington, A., McNab, I. R. & Montgomerie, C. A. 1989 *J. Phys.* B **22**, 3551–3586.

Carrington, A., McNab, I. R. & West, Y. D. 1993 *Mol. Phys.* **98**, 1073–1092.

Chambers, A. V. & Child, M. S. 1988 *Mol. Phys.* **65**, 1337–1344.

Cox, S. G., Critchley, A. D. J., McNab, I. R. & Smith, F. E. 1999 *Meas. Sci. Technol.* **10**, R101–R128.

Gentry, W. R., McClure, D. J. & Douglass, C. H. 1975 *Rev. Sci. Instrum.* **46**, 367.

Peko, B. L. & Champion, R. L. 1997 *J. Chem. Phys.* **107**, 1156–1162.

Pfeiffer, R. & Child, M. S. 1987 *Mol. Phys.* **60**, 1367–1378.

McNab, I. R. 1995 *Adv. Chem. Phys.* **89**, 1–87.

Miller, S., Tennyson, J. & Sutcliffe, B. T. 1989 *Mol. Phys.* **66**, 429–456.

Quack, M. 1977 *Mol. Phys.* **34**, 477–504.

Softley, T. P., MacKenzie, S. R., Merkt, F. & Rolland, D. 1997 *Adv. Chem. Phys.* **101**, 667–699.

Uy, D., Cordonnier, M. & Oka, T. 1997 *Phys. Rev. Lett.* **78**, 3844–3847.

Wolniewicz, L. 1983 *J. Chem. Phys.* **78**, 6173–6181.

Yousif, F. B., Hinojosa, G., de Urquijo, J., Cisneros, C. & Alvarez, I. 1997 *Int. J. Mass Spectrom. Ion. Proc.* **171**, 127–134.

Discussion

J. B. A. Mitchell (*PALMS, Université de Rennes, France*). What is the percentage of the 'visible H_3^+' that you see compared with your total beam current?

I. R. McNab. The percentage of H_3^+ ions involved in the whole spectrum is not a quantity that can be directly measured, but we can make a sensible estimate. A typical H_3^+ beam current in this experiment would be equivalent to 3.6×10^{11} ions per second, and for the strongest H_3^+ transitions we can measure the H^+ current directly while the transition is saturated, and this corresponds to 10^5 ions per second, so the fraction of the total population in a single initial level is 3×10^{-7} of the total H_3^+ beam. To calculate the total beam fraction involved in the observed spectrum we must estimate the number of initial states involved in the spectrum; we have approximately 27 000 transitions, and the maximum number of states that could be involved allowing for a selection rule on total angular momentum (and parity) is about 14 000. If we assume that all the states involved have an equal population,

this would give an upper limit for the percentage of the H_3^+ beam involved in the spectrum as 0.4%. Depending on the assumptions made in such calculations, we can estimate the percentage of the H_3^+ beam involved in the spectrum to between 1% and 0.01%. However, it is important to realize that the spectrum (and, hence, the population of the 'visible' H_3^+ states) can be completely quenched by using high pressures in the ion source (as would be expected).

PHILOSOPHICAL TRANSACTIONS OF THE ROYAL SOCIETY A MATHEMATICAL, PHYSICAL & ENGINEERING SCIENCES